Received: 8 February 2023 | Revised: 5 June 2023 | Accepted: 8 July 2023

DOI: 10.1111/exsy.13409

ORIGINAL ARTICLE

Expert Systems WILEY

Integrated recovery system with bidding-based satisfaction: An adaptive multi-objective approach

Huifen Zhong[1,2] | Zhaotong Lian[1] | Tianwei Zhou[2,3] | Ben Niu[2,3,4] | Bowen Xue[2]

[1]Faculty of Business Administration, University of Macau, Macau, China

[2]College of Management, Shenzhen University, Shenzhen, China

[3]Great Bay Area International Institute for Innovation, Shenzhen University, Shenzhen, China

[4]Institute of Big Data Intelligent Management and Decision, Shenzhen University, Shenzhen, China

Correspondence
Tianwei Zhou, College of Management, Shenzhen University, Shenzhen, China.
Email: tianwei@szu.edu.cn

Funding information
National Natural Science Foundation of China, Grant/Award Numbers: 71971143, 62103286; Humanities and Social Sciences Youth Foundation; Ministry of Education of the People's Republic of China, Grant/Award Number: 21YJC630181; University of Macau, Grant/Award Number: MYRG2019-00031-FBA; Guangdong Provincial Philosophy and Social Sciences Planning Project, Grant/Award Numbers: GD22CGL35, GD22XGL22; Special Projects in Key Fields of Universities in Guangdong Province, Grant/Award Number: 2022ZDZX2054; Guangdong Province Innovation Team, Grant/Award Number: 2021WCXTD002; Basic and Applied Basic Research Foundation of Guangdong Province, Grant/Award Number: 2019A1515110401; Natural Science Foundation of Guangdong Province, Grant/Award Number: 2020A1515010752; Natural Science Foundation of Shenzhen City, Grant/Award Number: JCYJ20190808145011259

Abstract

Efficient management of aircraft and crew recovery system is crucial for cost savings and improving the satisfaction, which are related to the airline's reputation. However, most existing work considers only one objective of minimizing costs or maximizing satisfaction. In this study, we propose a new integrated multi-objective recovery system that takes both cost and satisfaction into account simultaneously. To better capture crew satisfaction in the event of airport closure, a bidding mechanism for early off-duty task is designed. To overcome the experience-dependent and labour-consuming problems associated with current manual or mathematical recoveries, we develop an intelligent optimizer based on multi-swarm and MOPSO frameworks, termed adaptive seeking and tracking multi-objective particle swarm optimization algorithm (ASTMOPSO). Specifically, during the evolutionary process, the sub-swarm size undergoes adaptive internal transfer while executing more efficient evolutionary strategies to approach the global Pareto front. Additionally, five ad-hoc repair procedures are designed to ensure feasibility for our aircraft and crew recovery system. The ASTMOPSO is applied to real-world instances from Shenzhen Airlines with different sizes. Experimental results demonstrate the statistical superiority of our method over other popular peer algorithms. And the infeasible solution repair procedures significantly improve the feasibility rate by at least 40%, particularly for large-scale instances.

KEYWORDS
crew satisfaction, infeasible solution repair procedures, integrated aircraft and crew recovery system, multi-objective optimization, particle swarm optimization

1 | INTRODUCTION

The recovery system plays a crucial role in the airline industry, which is primarily divided into three stages: aircraft, crew, and passenger recoveries (Su et al., 2021). It aims to reschedule resources for flights deviating from their original plans (Erdem et al., 2021). The division of the recovery system is driven by the complexity of the integrated case and the existence of multiple diverse objectives and constraints. Recognizing that aircraft

and crew are valuable and controllable resources for airlines, this paper specifically focuses on addressing the integrated aircraft and crew recovery problem (I-ACRP).

To address the I-ACRP effectively, it is essential to first formulate the problem model and then design methods for its solution. Due to complex qualification and time limitation constraints on crew, problem of integrating crew and aircraft recovery is still in its infancy. According to Hassan et al. (2021), only four studies have focused on this integrated problem since 2009. Many models primarily aim to minimize recovery costs from the perspective of airlines. Le and Wu (2013) considered minimizing aggregate cost, which comprised of delay cost, cancellation cost, and assignment cost. Zhang et al. (2015) and Maher (2016) had similar cost minimization objective, but they also took the connection disruption penalty and cost of crew deadheading into account, respectively. More recently, Khiabani et al. (2022) also concentrated on cost minimization, but their main contribution lies in formulating the recovery model based on individual flight legs. In terms of passenger satisfaction, For the satisfaction considered aspect, Aguiar et al. (2011) tried to maintain the schedule as planned.

The existing works primarily focus on a single objective perspective, which has certain limitations in practical applications. Firstly, the obtained scheduling scheme may perform well in one objective but exhibit poor performance in other perspectives, leading to impractical recovery plans (Chen et al., 2013). Second, relying on a single solution cannot accommodate the diverse decision preferences of different decision-makers, thus lacking comprehensiveness (Atencia et al., 2019; Azouz & Boughaci, 2022). Furthermore, these previous works allocate less attention to the crew aspect, despite evidence demonstrating the significant impact of crew satisfaction on service quality and passenger loyalty, particularly during the COVID-19 pandemic (Nayak et al., 2022), even though it may cause economic loss from airline perspective.

Based on the considerations mentioned above, we propose a new multi-objective model for the integrated aircraft and crew recovery problem (referred to as I-MACRP) that simultaneously considers recovery cost and crew satisfaction, focusing on the scenario of airport closure disruptions. During the closure period, no activities are permitted, resulting in severe knock-on effects on subsequent flights, related aerodromes, and stakeholder emotions (Cook et al., 2009; Wu & Caves, 2002). Herein, cost objective refers to minimize the recovery cost for both aircraft and crew. To broaden the scope of potential recovery options and facilitate timely arrival of disrupted flights at their destinations before airport closing time, we also include the consideration of additional fuel cost, taking into account the ability to safely accelerate within a margin of 10% (Arıkan et al., 2017). Regarding crew satisfaction, we adopt a fairness approach commonly used in the aviation industry. Various measures have been employed to depict crew satisfaction, including seniority-based priority (Gamache et al., 1998), destination preference (Maenhout & Vanhoucke, 2010), and minimal conflict with preferred schedules (Zhou et al., 2020). To alleviate the waiting anxiety caused by airport closures and enhance satisfaction, this study places emphasis on ensuring fairness in crew on-duty time and rational arrangement of the earliest off-duty tasks. To achieve this, a bidding mechanism, which has been proven effective in achieving a certain degree of fairness and satisfaction (Quesnel et al., 2022), is newly incorporated to characterize crew satisfaction in this study.

The I-MACRP model is a challenging combinational optimization problem with complex constraints and multiple objectives, it is important to choose a suitable solution optimizer. In contrast to existing approaches that employ two-stage iterative heuristic decomposing the integrated problem into iterative sequential decisions Benders' decomposition method that transfers the original large-scale problem to a simplified master problem and subproblems (Khiabani et al., 2022), we focus on an integrated manner to obtain acquire a set of non-dominated solutions in a single run using an intelligent optimization algorithm. It can also overcome the limitations of sub-optimal, experience-dependent and labour-consuming problems associated with existed methods or manual recovery in realistic. According to Hassan et al. (2021), heuristic methods have been extensively used in aircraft recovery problems, constituting over 80% of publications in aviation disruption management literature from 2009 to 2020. Among these heuristic methods (Del Ser et al., 2019 for review), multi-objective particle swarm optimization (MOPSO, Coello et al., 2004) has gained popularity for its simplicity in addressing complex continuous or combinational optimization problems (Ben Ammar et al., 2020; Dou et al., 2021; Tan et al., 2021; Zomorodi-Moghadam et al., 2021). Hence, we design our optimizer based on the MOPSO algorithm. Since the original MOPSO is designed for continuous problems and may not be efficient for solving our I-MACRP, we design an ad-hoc matrix hybrid encoding scheme and develop some problem characteristic-based evolutionary strategies, such as adaptive multi-swarm division and symmetrical re-arrangement on the crew arrangement, to help for approaching the global Pareto front. Considering the strict compliance requirements of the aviation industry with various laws and regulations, which result in a sparse feasible solution space, we propose some corresponding recovery procedures for infeasible solutions in the aircraft crew integration system. These procedures aim to enhance the computational efficiency of the intelligent algorithm and increase the feasibility rate of the model.

To sum up, the main contributions of this study are listed below:

- Diverging from conventional single-objective models, we introduce a novel multi-objective recovery model that integrates both cost and crew satisfaction factors. Focusing on airport closure scenarios, a new method for depicting crew satisfaction, which encompasses a bidding mechanism for the earliest off-duty task and the fairness for on-duty time, is designed.
- We develop a novel intelligent optimization algorithm, ASTMOPSO, for solving the I-MACRP, which generates a set of nondominated solutions in a single run. To enhance detection efficiency, evolutionary strategies such as adaptive multi-swarm division and symmetrical re-arrangement of the crew, are designed to help for approaching the global Pareto front.

- A series of customized infeasible solution recovery procedures, specifically tailored for the complex and highly constrained aircraft-crew integrated recovery model, are designed and incorporated into the solution process. These approaches have been proven efficient in enhancing the computational efficiency of intelligent algorithm and feasibility rate of the model.

The remainder of the paper is organized as follows. In Section 2, we first introduce the formulation of the proposed I-MACRP model. Section 3 details our ASTMOPSO algorithm and its coding strategies. Section 4 reports the experimental results and specific recovery schemes. Finally, conclusions and future works are discussed in Section 5.

2 | PROBLEM DESCRIPTION AND MODEL CONSTRUCTION

2.1 | Problem description

Considering the dramatic flight decrease during the COVID-19 epidemic, our recovery focuses on the economic situation, where the final flight returns to its departure airport within one operational day without considering overnight crew costs, aircraft parking costs, and so forth. Moreover, it is assumed that aircraft for each flight is already settled, which aligns with the practical situation.

The earliest off-duty flight task is competed by a bidding mechanism. During bidding procedure, each crew team gives bidding score, yielding a winner with the maximized bidding score (Achour et al., 2007). Figure 1a is an illustrative example with bidding scores (3, 8, and 5 for crew C_1, crew C_2, and crew C_3, respectively). Based on the bidding principle, crew C_2 with the highest score, is the bidding winner. And the yellow flight task executed by crew C_1 is the subject of the bidding with the earliest off-duty time 18:45. According to the bidding setting, these two crews should exchange their duties directly. Besides, Figure 1b exhibits the benefit of cruise speed control action in an airport closure situation. It is clear that the recovery scheme considering cruise speed control (blue dotted line) can save 120-min delay time than the case without cruise speed control (orange dotted line).

To recover aircraft and crew from irregular disruption, we mainly apply the following recovery operations: 1) cancelling flight, 2) delaying flight, 3) calling up reserved crew, 4) swapping crew, and 5) controlling cruise speed. The first four methods are the most commonly used approaches (see reviews by Su et al., 2021, and Hassan et al., 2021), while the fifth one is a newly introduced and flexible approach in this paper. It effectively reduces the waiting time caused by airport closure, albeit at the expense of increased dimensionality in the model's solution space. It should be noted that each crew only has one type of licence; the exchange should occur between crews with the licence for same aircraft type.

2.2 | Model construction

The regulations and constraints in different countries may be various. Our model here is based on the latest government document in China. For reading convenience, Table 1 firstly provides a summary of the notations used in our I-MACRP formulation, in which **available parameters** are input for a particular instance, and **decision variables** are the final purpose of our recovery operation. Expressly, overline and underline parameters represent the upper boundary and schedule value, respectively.

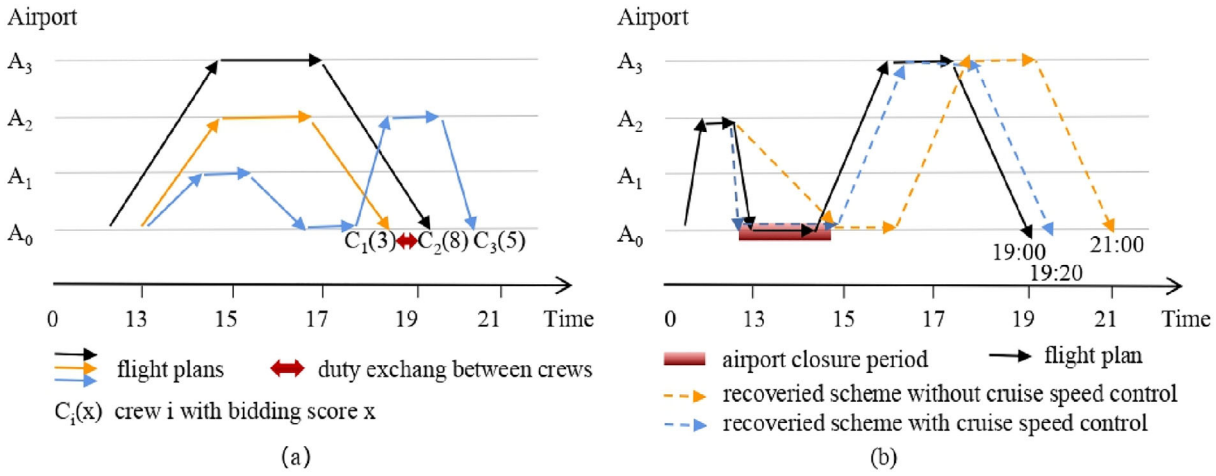

FIGURE 1 Illustration example. (a) bidding mechanism; (b) cruise speed control effect.

TABLE 1 Summary of notations.

Available parameters:			
t_b	Begin time of airport to be closed	t_e	End time of airport to be reopened
$\widetilde{t}_b$	Begin time of other airlines occupying	$\widetilde{t}_e$	End time of other airlines occupying
S	Set of disturbed strings s	$J(s)$	Set of disturbed flights in string s
R	Set of all kinds of crew, indexed by r	E	Set of aircraft types e
R^o	Set of all disturbed on-duty crews r^o	R^{re}	Set of all reserve crews r^{re}
$R^o(e)$	Set of on-duty crews of aircraft e	$R^{re}(e)$	Set of reserve crews of aircraft e
$K(r)$	Set of flights that crew r executed	$f_{r,k}$	k^{th} on-duty flight of crew r
$f_{s,j}$	j^{th} disturbed flight in flight string s	$\underline{t}^d_{f_{s,j}}$	Scheduled departure time of $f_{s,j}$
$\underline{t}^f_{f_{s,j}}$	Scheduled flying time of flight $f_{s,j}$	$\underline{t}^i_{f_{s,j}}$	Scheduled arrival time of flight $f_{s,j}$
$\underline{v}_{f_{s,j}}$	Scheduled cruise speed of flight $f_{s,j}$	$d_{f_{s,j}}$	Cruise distance of flight $f_{s,j}$
$\underline{r}_{f_{s,j}}$	Scheduled crew arrangement for $f_{s,j}$	$a^d_{f_{s,j}}$	Departure airport of flight $f_{s,j}$
$a^i_{f_{s,j}}$	Arrival airport of flight $f_{s,j}$	$r^w(e)$	Winner crew for aircraft type e
$\underline{s}^w$	Scheduled on-duty string of winner	s^b	Bided string that off-duty earliest
$\underline{t}^g$	Minimal ground turn-around time	$\overline{t}^l$	Maximal delay time for flight
$\overline{t}^{rf}$	Maximal crew daily on-fly time	$\overline{t}^{ro}$	Maximal crew daily on-duty time
$\gamma^{s^b}_{f_{s,j}}$	Parameter with a value of 1 if $f_{s,j}$ belongs to s^b and 0 otherwise		
$\theta^r_{f_{s,j}}$	Parameter with a value of 1 if crew r is qualified for $f_{s,j}$ and 0 otherwise		
S^p	Subset of disturbed string set S by eliminating strings $\underline{s}^w$ and s^b		
M	Set of flights that overlap with $f_{s,j}$, which is made up of flight m whose timetable satisfies: $t^d_{f_{s,j}} < t^d_m < t^i_{f_{s,j}}, t^d_m < t^d_{f_{s,j}} < t^i_m, t^d_{f_{s,j}} < t^d_m < t^i_m < t^i_{f_{s,j}}$ or $t^d_m < t^d_{f_{s,j}} < t^i_{f_{s,j}} < t^i_m$.		
c_n	Unit costs, where $c_n, n = 1,2,3,4,5$ represent unit cost of cancelling flight(¥), delaying flight(¥/min), calling reserve crew(¥), swapping crew(¥), and jet fuel(¥/kg)		
$q_n(e)$	Cruise fuel coefficients of aircraft e, where $q_n, n = 1,2,3,4$ represent aircraft drag and fuel consumption coefficients, air density at given altitude, and gravitational acceleration		
Decision variables:			
$z_{f_{s,j}} \in \{0,1\}$	Whether flight $f_{s,j}$ is cancelled. 1: cancelled; 0: not cancelled		
$t^d_{f_{s,j}} \in \left[\underline{t}^d_{f_{s,j}}, \underline{t}^d_{f_{s,j}} + \overline{t}^l\right]$	Recovered departure time of flight $f_{s,j}$		
$v_{f_{s,j}} \in \left[\underline{v}_{f_{s,j}}, \underline{v}_{f_{s,j}} \times (1+10\%)\right]$	Recovered cruise speed of flight $f_{s,j}$		
$r_{f_{s,j}}(e) \in \{R(e) \cup R^{re}(e)\}$	Recovered crew arrangement for flight $f_{s,j}$ of aircraft e		

We follow flight string representation Petersen et al. (2012) to represent our problem. A flight string is a sequence of flights with timing decisions, which has advantage in handling complicated constraints such as ground turn-around time restriction depending on the sequence of flights. In our model, $\left(\underline{t}^d_{f_{s,j}}, \underline{t}^f_{f_{s,j}}, \underline{v}_{f_{s,j}}, d_{f_{s,j}}, \underline{r}_{f_{s,j}}, a^d_{f_{s,j}}, a^i_{f_{s,j}}\right)$ represents the available attributes of flight $f_{s,j}$ and $\left(z_{f_{s,j}}, t^d_{f_{s,j}}, v_{f_{s,j}}, r_{f_{s,j}}\right)$ is its decision variable attributes. Before introducing the complete mathematical formulation, we first explain three pre-defined representations used for easy reading. $I_{\{.\}}$ is an indicator function that equals 1 if it satisfies the condition in parentheses and 0 otherwise. $A \backslash A_1$ represents the operation that eliminates subset A_1 from its original set A. And $num(.)$ represents the operation that counts the number in the set. Notably, we can also represent another specific flight by changing the subscript. For example, $t^d_{f_{r,num(K(r))}}$ is the departure time of the last on-duty flight of crew r, and $\underline{t}^f_{f_{r,num(K(r))}}$ is the scheduled flying time of the final on-duty flight of crew r, and so forth. The detailed objectives and constraints of our I-MACRP model are given as follows:

$$\min f_1 = \sqrt{\frac{\sum_{r \in R^o}\left(\left(t^i_{f_{r,num(K(r))}} - t^d_{f_{r,1}}\right) - \frac{\sum_{r \in R^o}\left(t^i_{f_{r,num(K(r))}} - t^d_{f_{r,1}}\right)}{num(R^o)}\right)^2}{num(R^o)}} \tag{1}$$

$$\min f_2 = \sum_{s\in S}\sum_{j\in J(s)} c_1 z_{f_{s,j}} + \sum_{s\in S}\sum_{j\in J(s)} c_2\left(1-z_{f_{s,j}}\right)\left(t^d_{f_{s,j}} - \underline{t}^d_{f_{s,j}}\right) + \sum_{s\in S^p}\sum_{j\in J(s)} c_3 \cdot I_{\left\{r_{f_{s,j}}\in R^{re}\right\}} + \sum_{s\in S^p}\sum_{j\in J(s)} c_4 I_{\left\{r_{f_{s,j}}\neq \underline{r}_{f_{s,j}}\right\}} I_{\left\{f_{s,j}\notin R^{re}\right\}} + \sum_{s\in S}\sum_{j\in J(s)} c_5\left(F\left(v_{f_{s,j}}\right) - F\left(\underline{v}_{f_{s,j}}\right)\right) \tag{2}$$

$$I_{\left\{t^d_{f_{s,j}}\neq\emptyset\right\}} + z_{f_{s,j}} = 1,\ \forall s\in S, \forall j\in J(s) \tag{3}$$

$$\left(t^d_{f_{s,j}} - t_e\right)\left(t^d_{f_{s,j}} - t_b\right) > 0, \forall s\in S, \forall j\in J(s) \tag{4}$$

$$\left(t^i_{f_{s,j}} - t_e\right)\left(t^i_{f_{s,j}} - t_b\right) > 0,\ \forall s\in S, \forall j\in J(s) \tag{5}$$

$$\left(t^d_{f_{s,j}} - \widetilde{t}_e\right)\left(t^d_{f_{s,j}} - \widetilde{t}_b\right) > 0,\ \forall s\in S, \forall j\in J(s) \tag{6}$$

$$\left(t^i_{f_{s,j}} - \widetilde{t}_e\right)\left(t^i_{f_{s,j}} - \widetilde{t}_b\right) > 0,\ \forall s\in S, \forall j\in J(s) \tag{7}$$

$$\theta^r_{f_{s,j}} \cdot \left(I_{\left\{r_{f_{s,j}}\neq\emptyset\right\}} + z_{f_{s,j}}\right) = \theta^r_{f_{s,j}},\ \forall s\in S, \forall j\in J(s) \tag{8}$$

$$r_{f_{s,j}} \neq r_m,\ \forall s\in S, \forall j\in J(s), \forall m\in M \tag{9}$$

$$\sum_{s\in S}\sum_{j\in J(s)} I_{\left\{r_{f_{s,j}}\in R^{re}(e)\right\}} \le num(R^{re}(e)),\ \forall e\in E \tag{10}$$

$$a^i_{f_{s,j}} = a^d_{f_{s,j+1}},\ \forall s\in S, \forall j\in J(s)\backslash\{num(J(s))\} \tag{11}$$

$$t^d_{f_{s,j+1}} - t^i_{f_{s,j}} \ge \underline{t}^g,\ \forall s\in S, \forall j\in J(s)\backslash\{num(J(s))\} \tag{12}$$

$$t^d_{f_{r,k+1}} \ge t^i_{f_{r,k}},\ \forall r\in R, \forall k\in K(r)\backslash\{num(K(r))\} \tag{13}$$

$$t^i_{f_{r,num(K(r))}} - t^d_{f_{r,1}} \le \overline{t}^{ro},\ \forall r\in R \tag{14}$$

$$\sum_{s\in S}\sum_{j\in J(s)} I_{\left\{r_{f_{s,j}}=r\right\}} \cdot \left[\underline{t}^f_{f_{s,j}} - \left(\frac{d_{f_{s,j}}}{\underline{v}_{f_{s,j}}} - \frac{d_{f_{s,j}}}{v_{f_{s,j}}}\right)\right] \le \overline{t}^{rf},\ \forall r\in R \tag{15}$$

$$a^d_{f_{r,1}} = a^i_{f_{r,num(K(r))}},\ \forall r\in R \tag{16}$$

$$\gamma^{s^b}_{f_{s,j}} \cdot r_{f_{s,j}} = \gamma^{s^b}_{f_{s,j}} \cdot r^w(e),\ \forall s\in S, \forall j\in J(s) \tag{17}$$

$$r_{f_{\underline{s}^w j}} = r_{f_{s^b,1}},\ \forall j\in J(\underline{s}^w) \tag{18}$$

where $t^i_{f_{r,num(K(r))}} = t^d_{f_{r,num(K(r))}} + \left(\underline{t}^f_{f_{r,num(K(r))}} - \left(\frac{d_{f_{r,num(K(r))}}}{\underline{v}_{f_{r,num(K(r))}}} - \frac{d_{f_{r,num(K(r))}}}{v_{f_{r,num(K(r))}}}\right)\right)$ in formulas (1) and (14) is the actual final off-duty time of crew r, in which the largest bracket indicates the time saved by speeding up (Similarly, $t^i_{f_{s,j}}$ in formulas (5), (7), (12) means actual arrival time of flight $f_{s,j}$ and $t^i_{f_{r,k}}$ in formulas (13) represents the actual arrival time of k^{th} on-duty flight of crew r), $S^p = S\backslash\{\underline{s}^w, s^b\}$ in formulas (2) is a subset after eliminating strings $\underline{s}^w$ and s^b from set S, and $F\left(v_{f_{s,j}}\right) = q_1(e)v^2_{f_{s,j}} + q_2(e)v_{f_{s,j}} + \frac{q_3(e)}{v^2_{f_{s,j}}} + \frac{q_4(e)}{v^3_{f_{s,j}}}$ in formula (2) is total fuel consumption at cruise speed $v_{f_{s,j}}$ (similar meaning of $F\left(\underline{v}_{f_{s,j}}\right)$ with speed $\underline{v}_{f_{s,j}}$). Since $v_{f_{s,j}}$ is consistently greater than the schedule $\underline{v}_{f_{s,j}}$, which represents the minimum fuel cost, the last component in equation (2) will always yield a positive value.

The first two objectives focus on satisfaction and cost from the perspective of crew members and airlines, respectively. Objective function (1) guarantees crew satisfaction, which is reflected by the minimized standard deviation of duty time among all on-duty crews. Objective function (2) represents the total recovery costs, which consist of five parts: (i) cancellation costs; (ii) delay costs; (iii) reserve crew calling costs; (iv) crew swapping costs and (v) additional fuel costs due to cruise speed increase. The computational formula between fuel costs and cruise speed can be acquired in Poles (2009) and the details for 399 aircraft types are available in Nuic (2010).

Constraint (3) promises that each flight is cancelled or reassigned to a new departure time. Constraints (4)–(7) ensure no take-off and landing activities during the airport shutdown and occupied periods. Here, occupied period reflects recovery priority, which making our model more realistic. Constraint (8) promises that each flight is cancelled or reassigned to a qualified crew. Constraint (9) stipulates that each crew cannot be assigned more than two flights simultaneously, where r_m is the crew arrangement for flight $m, m \in M$. Constraint (10) is the capacity constraint on the reserve crew. Constraints (11)–(12) guarantee spatial cohesion and minimal ground turn-around time request between two connective flights. Constraint (13) prevents the crew's subsequent duty from working before the completion time of his/her primary duty. Constraints (14)–(15) ensure that the crew's daily cumulative on-duty and flying times should not exceed their distinct boundaries. It is strictly regulated for flight safety. Constraint (16) ensures all crews return to their departure airport on their final duty. Constraint (17) represents the bidding winner to execute all flights in the earliest off-duty flight string. Constraint (18) requires winner's scheduled duty to be rearranged to the planned crew that performs the earliest off-duty string. Constraints (17)–(18) are the main constraints of the bidding mechanism, which have been explained in detail in Section 2.1.

3 | SOLUTION PROCEDURE BASED ON ASTMOPSO ALGORITHM

As stated by Hassan et al. (2021), the quality of solutions depends on the heuristics ability to adapt to a particular problem. To efficiently solve the I-MACRP model aforementioned above, this part comprehensively proposes a new ad-hoc ASTMOPSO algorithm, followed by an example to understand the specific coding strategies, that is, decision variable representations.

3.1 | ASTMOPSO algorithm

The procedure of ASTMOPSO is illustrated in Figure 2, aiming to generate an external repository Archive A that stores all non-dominated solutions. The particle population is initialized as A_{pop}. Dominant relationship, as defined by Deb et al. (2002), determines whether a new solution is added to the A or if existing elements in the A are discarded. Whole population undergoes an evolution state-based swarm division strategy, where particles progressively move from the seeking swarm to the tracking swarms. Two detection strategies, based on problem characteristics, are randomly executed a predetermined number of times for each particle in the seeking swarm S_{pop}, thereby enhancing the global diversity of the population. And the best solution optimization learning strategy (Coello et al., 2004) is implemented in the tracking swarm T_{pop} to facilitate efficient local search. To ensure feasibility, five repair procedures are activated for all evolved infeasible solutions. During each evolution, the first $num(A_{pop})$ solutions, ranked in ascending order based on Pareto front ranking, are selected as offspring to maintain the primary population size. The three components with a blue background (i.e., Components 2, 3 and 5) are our main contributions, which are described in detail as follows:

(1) Evolution state-based swarm division strategy. Global detection and careful local search are two important operations that help increase solution diversity and accuracy, respectively. In most existing works, update relies on global optimization information. In fact, at the beginning stage with small iteration t, the solutions found are still far away from the actual Pareto front; thus, it is better to allocate more computing resources to make extensive explorations. In each iteration t, whole population A_{pop} will be adaptively divided into seeking swarm S_{pop} and tracking swarm T_{pop} as Equations (19)–(20). When t is small, more particles will execute seeking process to expand solution diversity. As t increases, population focuses on careful local search. The specific calculations are given as follows:

$$S_{pop} = \bigotimes \left(A_{pop}, floor\left(N \cdot \left[r_s^{\max} - \left(r_s^{\max} - r_s^{\min} \right) \cdot \frac{t}{T_{\max}} \right] \right) \right), \tag{19}$$

$$T_{pop} = C_{A_{pop}} S_{pop} = \{ i | i \in A_{pop}, \text{and } i \notin S_{pop} \} \tag{20}$$

where $r_s^{\max}$ and $r_s^{\min}$ represent the boundary rate of S_{pop} among the whole population. $floor(.)$ denotes a round-down operator. And $\bigotimes(M,n)$ is a pre-defined symbol which means randomly choosing n elements from a set M.

(2) Two novel detection mechanisms for particles in seeking swarm S_{pop}. Detection operation is necessary to guarantee a wide-range solution set, directly determining the solution quality. To guarantee seeking effectiveness, two problem-characteristics-based disruption mechanisms are designed. First, we randomly choose a sub-dimension decision variable to execute acceptable re-assignment. Second, considering that the

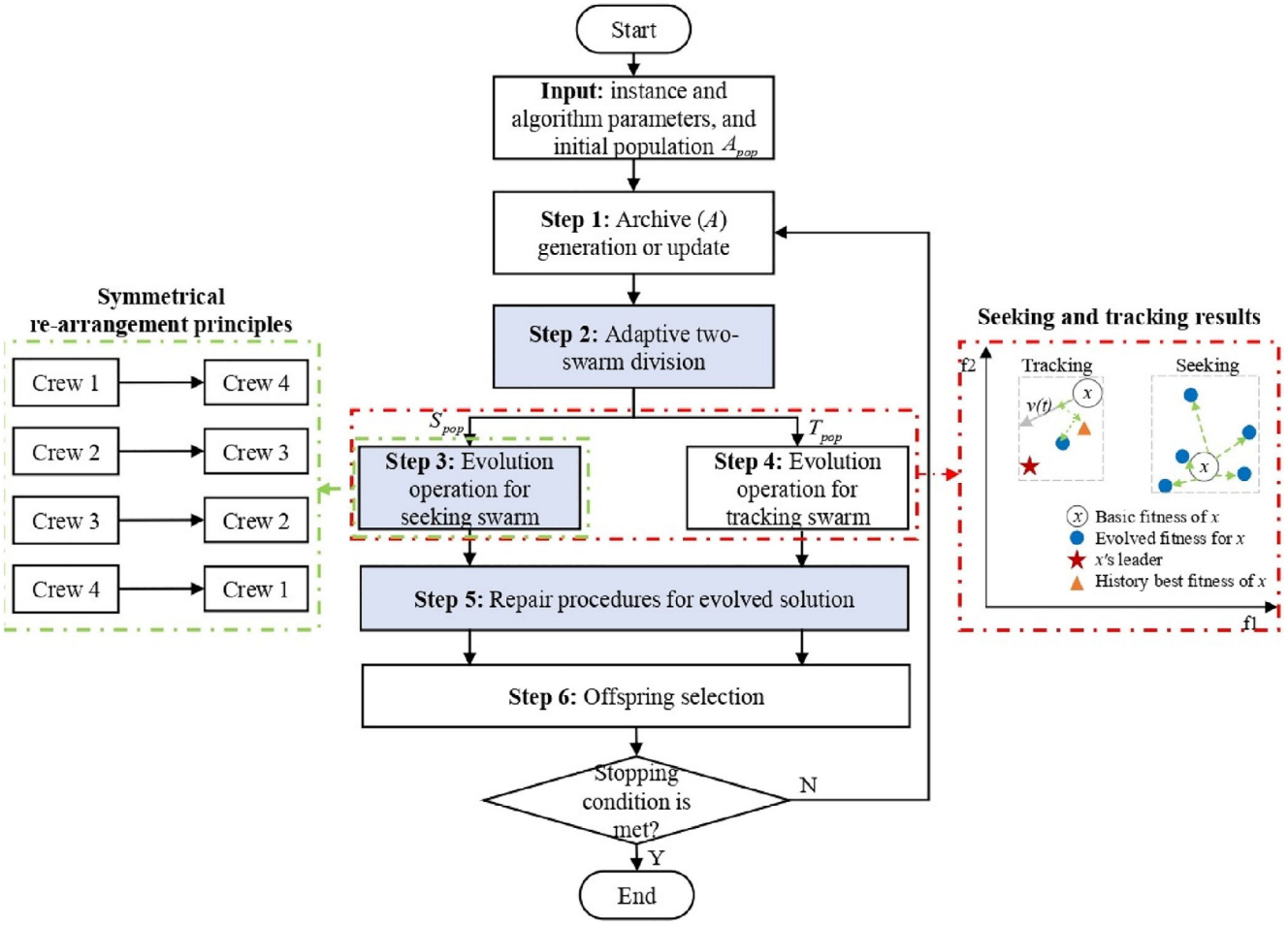

FIGURE 2 Main procedure of the ASTMOPSO algorithm.

crew decision variable directly affects objectives 1 and 2 in I-MACRP, we perform symmetrical re-arrangement on the crew. Equation (21) gives the specific formulations of seeking operation for the j^{th} memory pool of particle i.

$$x_i(t+1)_j = \begin{cases} x_{i,sd}(t) + U_{sd} \cdot \times \bigoplus(1, N_{sd}), & \text{if } rand < 1/2 \\ U_{crew} - x_{i,crew}(t) + L_{crew}, & \text{otherwise} \end{cases} \tag{21}$$

where sd is a sub-vector selected randomly. Vector $crew$ is made up of all crew arrangements. U_{sd} represents corresponding maximum for the elements among vector sd. U_{crew} and L_{crew} are the maximum and minimum for the elements among vector $crew$, respectively. $M \cdot \times N$ and $\bigoplus(m,n)$ are two pre-defined symbols, which represent operation of multiplying the corresponding elements between matrices M and N, and generating a matrix with m row and n columns obeying standard normal distribution, respectively. And $rand \sim U(0,1)$ is a random number.

(3) Problem characteristics-based repair procedures for the evolved infeasible solution. The I-MACRP model defined in Section 2.2 is a complex, constrained multi-objective problem, which has difficulty in finding feasible solutions by evolution operation directly. When an evolved solution is generated, the following infeasible solution repair procedures will be activated by considering problem characteristics and other repair techniques proposed by Jordehi (2015). The specific infeasible solution repair procedures are concluded as follows:

- **Repair procedure 1.** In a realistic problem, each decision variable has its corresponding value range to satisfy the real significance. For each dimension x_i in decision variable $x = (x_1, x_2, \ldots, x_i, \ldots, x_n)$, if x_i is smaller than its low boundary L_i, we set $x_i = L_i$, and if x_i exceeds its upper boundary U_i, we set $x_i = U_i$.
- **Repair procedure 2.** The randomness of the algorithm will cause a high violation probability of constraint (9). We define a set X_{avai} to store the available crews associated with an aircraft type so far. For the crew with more than two tasks at once, we execute the tasks using the element in X_{avai} sequentially until constraint (9) is met.

- **Repair procedure 3.** In I-MACRP model, ground turn-around time is required for passengers to get up, drop off, or disinfect during the COVID-19 epidemic. If constraint (12) is violated, we postpone the departure time of subsequent flight until the needed ground turn-around time is met.
- **Repair procedure 4.** If crew's subsequent duty is earlier than his/her preceding completion time, we postpone the departure time of the latter duty to guarantee feasibility.
- **Repair procedure 5.** In I-MACRP model, no departure or arrival activities are allowed during the airport shutdown and occupied period. If a flight arrives at the airport during the illegal period (i.e., constraints (5) or (7) is violated), we randomly increase cruise speed or postpone its departure time. Similar repair procedures can be applied to the cases that a flight departs during the unallowed period.

3.2 | Coding strategy

This sub-part introduces elaborate coding strategies to fit the I-MACRP model well. Since the value of the cancellation decision variable $z_{f_{s,j}}$ can be known easily if the delay time satisfies $\Delta_t \geq 480$ (480 min is the maximal delay time regulated in the document in China), the 4-dimension decision variables for each disturbed flight $f_{s,j}$ can be reduced to 3-dimension, that is, $\left(\Delta_t = t^d_{f_{s,j}} - \underline{t}^d_{f_{s,j}}, \Delta_v = v_{f_{s,j}} - \underline{v}_{f_{s,j}}, r_{f_{s,j}}\right)$. Table 2 explains solution representation using an instance with n disturbed strings. For example, $\Delta_t = 3$ in $f_{1,1}$ means that the scheduled first flight in string 1 will delay 3 min corresponding to its scheduled departure time; $\Delta_v = 0$ in $f_{n,4}$ represents that the scheduled 4^{th} flight in string n keeps its scheduled cruise speed; Assume $R^{re} = \{18, 19, 20, 21\}, r_{f_{s,j}} = 21$ in $f_{n,4}$ means that this flight calls for a reserve crew. For the discrete characteristics of Δ_t and $r_{f_{s,j}}$, a round-off number method is used on the related bits.

4 | EXPERIMENTAL STUDIES AND DISCUSSIONS

In this section, experiments are performed on real-world instances with peer algorithms to verify the superiority of ASTMOPSO in solving the I-MACRP. All experiments are implemented in Matlab R2020a on a PC with an Intel Core i5-8250U @ 1.80 GHz and 8.00 GB RAM.

4.1 | Test instances

Our real-world instances derived from Shenzhen Airlines in a single-day operation that suffered a 150-min closure at Shenzhen airport (we thank VariFlight company for providing the statistics of aircraft and crew as Table 3 shown). To test the universality of our solution method, we generate another two cases with different scales by adjusting closure time dynamically and given in the first two lines of Table 4. Case 1 includes 4 disturbed flight strings (16 disturbed flights) under 30-min closure time, representing a slight accident, such as a minor obstacle on the runway. Considering airport will try its best to shorten the closure time (Pejovic et al., 2009), a 60-min closure time with 36 disturbed flights is regarded as Case 2. It describes an off-season situation when the airline industry is in a recession. Finally, the realistic Case 3 with a 150-min closure time shows a case suffering extreme weather or the severe outbreak of COVID-19.

Our I-MACRP model further considers crew satisfaction by allowing bidding for the earliest off-duty flight string. We randomly generate crews' bidding scores and obtain the corresponding bidding winners for different aircraft types (i.e., the A320 and B737). The random generator for bidding scores is reasonable because it is a known input that can be collected directly. Table 5 concludes the fuel cost parameters of two fleets by referencing Nuic (2010) and Arıkan et al. (2017). Two reserve crews are given for each fleet. Referring to the industry regulations, minimal ground turn-around time, maximal flight delay time, crew daily on-duty time, and on-flying time in our experiments are 40, 480, 1080, and 780 min. And the unit costs of delay, cancellation, calling for reserve crew, swapping crew, and jet fuel are set as 100, 100,000, 1000, 800, and 6.5, respectively.

TABLE 2 Example of the coding strategy for the I-MACRP model.

	Scheduled string 1								Scheduled string n						
	$f_{1,1}$			...	$f_{1,4}$			...	$f_{n,1}$			...	$f_{n,4}$		
Coding design	Δ_t	Δ_v	$r_{f_{s,j}}$	...	Δ_t	Δ_v	$r_{f_{s,j}}$	...	Δ_t	Δ_v	$r_{f_{s,j}}$	...	Δ_t	Δ_v	$r_{f_{s,j}}$
Position	3	0.9	1	...	65	0.04	8	...	0	0.1	19	...	490	0	21

TABLE 3 Instance details of Shenzhen Airlines provided by the VariFlight company.

s	e	$f_{s,j}$	$\underline{t}^d_{f_{s,j}}$ and $\underline{t}^i_{f_{s,j}}$	$a^d_{f_{s,j}}$ and $a^i_{f_{s,j}}$	$D_{f_{s,j}}$	$\underline{r}_{f_{s,j}}$
1	A320	$f_{1,1} \rightarrow f_{1,2} \rightarrow f_{1,3} \rightarrow f_{1,4}$	6:05–9:30 → 10:20–13:45 → 17:10–19:30 → 20:30–22:50	SZX → XNN → SZX → MIG → SZX	2244, 2244, 1303, 1303	1
2		$f_{2,1} \rightarrow f_{2,2} \rightarrow f_{2,3} \rightarrow f_{2,4}$	7:25–11:05 → 11:55–15:10 → 18:15–21:15 → 22:05–25:10	SZX → HFE → SZX → WXN → SZX	2464, 2100, 1882, 1955	2
3		$f_{3,1} \rightarrow f_{3,2} \rightarrow f_{3,3} \rightarrow f_{3,4}$	8:05–10:15 → 11:05–13:10 → 14:40–17:40 → 19:40–22:40	SZX → YBP → SZX → XIY → SZX	1158, 1086, 1882, 1882	3
4		$f_{4,1} \rightarrow f_{4,2} \rightarrow f_{4,3} \rightarrow f_{4,4}$	10:25–12:35 → 13:35–15:50 → 19:00–21:05 → 21:55–24:10	SZX → HFE → SZX → WXN → SZX	1158, 1231, 1086, 1231	4
5		$f_{5,1} \rightarrow f_{5,2} \rightarrow f_{5,3} \rightarrow f_{5,4}$	8:15–10:55 → 12:05–14:50 → 17:15–19:45 → 21:00–23:40	SZX → TNA → SZX → SZX → SZX	1593, 1665, 1448, 1593	5
6		$f_{6,1} \rightarrow f_{6,2} \rightarrow f_{6,3} \rightarrow f_{6,4}$	6:40–9:55 → 10:45–14:20 → 18:00–20:25 → 21:45–24:15	SZX → DLC → SZX → PVG → SZX	2100, 2389, 1376, 1448	6
7		$f_{7,1} \rightarrow f_{7,2} \rightarrow f_{7,3} \rightarrow f_{7,4}$	10:00–12:05 → 13:10–15:25 → 17:05–19:45 → 20:55–23:35	SZX → HGH → SZX → SZX → SZX	1086, 1231, 1593, 1593	7
8		$f_{8,1} \rightarrow f_{8,2} \rightarrow f_{8,3} \rightarrow f_{8,4}$	7:50–10:30 → 11:15–13:45 → 16:40–18:40 → 19:50–22:05	SZX → LJG → SZX → HGH → SZX	1593, 1448, 1014, 1231	8
9		$f_{9,1} \rightarrow f_{9,2} \rightarrow f_{9,3} \rightarrow f_{9,4}$	7:00–9:55 → 10:55–13:50 → 14:55–17:50 → 18:55–22:00	SZX → TAO → SZX → TNA → SZX	1810, 1810, 1810, 1955	9
10		$f_{10,1} \rightarrow f_{10,2} \rightarrow f_{10,3} \rightarrow f_{10,4}$	7:55–10:30 → 11:45–14:25 → 16:25–19:35 → 21:00–24:45	SZX → PVG → SZX → PEK → SZX	1520, 1593, 2027, 2534	10
11		$f_{11,1} \rightarrow f_{11,2} \rightarrow f_{11,3} \rightarrow f_{11,4}$	7:05–9:40 → 10:45–13:35 → 15:00–17:40 → 19:15–22:10	SZX → XIY → SZX → PVG → SZX	1520, 1738, 1593, 1810	11
12		$f_{12,1} \rightarrow f_{12,2} \rightarrow f_{12,3} \rightarrow f_{12,4}$	8:30–10:55 → 12:00–14:35 → 16:10–18:40 → 20:00–22:30	SZX → PVG → SZX → NKG → SZX	1376, 1520, 1448, 1448	12
13		$f_{13,1} \rightarrow f_{13,2} \rightarrow f_{13,3} \rightarrow f_{13,4}$	9:25–11:45 → 12:50–15:10 → 17:00–19:15 → 20:15–22:40	SZX → WXN → SZX → NGB → SZX	1303, 1303, 1231, 1376	13
14	B737	$f_{14,1} \rightarrow f_{14,2} \rightarrow f_{14,3} \rightarrow f_{14,4}$	9:10–11:15 → 12:00–13:55 → 15:40–18:50 → 19:50–23:10	SZX → XFN → SZX → TAO → SZX	1074, 931, 2005, 2148	16
15		$f_{15,1} \rightarrow f_{15,2} \rightarrow f_{15,3} \rightarrow f_{15,4}$	7:00–10:15 → 11:35–15:00 → 17:10–19:40 → 20:40–23:25	SZX → TSN → ZX → LYI → SZX	2076, 2220, 1432, 1647	17
16		$f_{16,1} \rightarrow f_{16,2} \rightarrow f_{16,3} \rightarrow f_{16,4}$	7:05–9:05 → 10:15–12:40 → 14:30–17:50 → 19:00–22:35	SZX → HGH → SZX → PEK → SZX	1002, 1360, 2148, 2363	18
17		$f_{17,1} \rightarrow f_{17,2} \rightarrow f_{17,3} \rightarrow f_{17,4}$	9:05–11:20 → 12:40–14:55 → 16:50–19:00 → 20:15–22:20	SZX → CKG → SZX → CKG → SZX	1217, 1217, 1146, 1074	19

Note: s, string number; →, symbol represents sequential order.

4.2 | Experimental parameter settings and performance metrics

To demonstrate the superiority of our algorithm in solving the aforementioned instances, the solution results are compared with some typical heuristic algorithms and improved heuristic algorithms in recent years, such as SPEA2 (Zitzler et al., 2001), MOPSO (Coello et al., 2004), MOEA/D (Zhang & Li, 2007), NSGA III (Deb & Jain, 2013), CMOPSO (Zhang et al., 2018), and MORBCO (Niu et al., 2021). To acquire fair and convincing results, each experiment runs 10 times independently with the same population size of 30 and maximum generations of 350. The key parameters

TABLE 4 Three different-scale airport closure cases.

Cases	Scales	Disturbed flights	Closure time	Closure period	Aircraft type	Bidding winners	Reserve crews
1	4	16	30 min	[13:45,14:15]	A320, B737	3 & 6	{4,5}&{7,8}
2	9	36	60 min	[13:45,14:45]		7 & 10	{8,9}&{12,13}
3	17	68	150 min	[13:45,16:15]		13 & 17	{14,15}&{20,21}

TABLE 5 Parameters of two fleet types used in calculating fuel cost.

e	$\underline{v}_{f_{sj}}$	$\overline{v}_{f_{sj}}$	q_1	q_2	q_3	q_4
A320	14.48	15.928	0.000025790	0.154734277	0.379117180	2274.703078
B737	14.32	15.752	0.002761029	0.049698524	0.049698524	1179.863088

which render each algorithm to perform best in the original literature are adopted, and the main details, including our ASTMOPSO algorithm, are listed as follows:

- In SPEA2, probabilities $P_{crossover} = 0.1$ and $P_{mutation} = 0.2$.
- Regarding MOPSO, learning factors $c_1 = 1$, $c_2 = 2$, and the inertia weight $w_0 = 0.9$, $w_1 = 0.5$.
- About MOEA/D, probability $P_{neighbor} = 0.15$.
- Considering NSGA-III, probabilities $P_{crossover} = 0.1$ and $P_{mutation} = 0.5$.
- With regard to CMOPSO, number $Elite_{num} = 10$.
- Concerning MORBCO, $N_{swim} = 4$, $c_1 = 3$, $c_2 = 3$, $Elite_{num} = 20$, and chemotaxis step $C = 0.001$.
- In ASTMOPSO, $c_1 = 1$, $c_2 = 2$, $N_{dt} = 5$, $N_{dd} = 5$, $w_0 = 0.9$, and $w_1 = 0.5$.

The vital aim of multi-objective optimization is to find a uniformly distributed subset (i.e., *PF*) that approximates the true Pareto-optimal front *PF** as close as possible. In this paper, we adopt three popular performance metrics to evaluate the solution quality of all compared algorithms, which include Spread (SP) (Deb et al., 2002), Hypervolume (HV) (Zitzler & Thiele, 1999), and Inverted Generational Distance (IGD) (Bosman & Thierens, 2003) as follows:

- $SP = \frac{\sum_{j=1}^{|o|} d_j^e + \sum_{i=1}^{|PF|} |d_i - \overline{d}|}{\sum_{j=1}^{|o|} d_j^e + |PF| \cdot \overline{d}}$ measures uniform distribution along obtained *PF*, where $|o|$ is objective numbers, d_j^e represents Euclidean distance between the extreme solution in the j-th objective direction and the corresponding extreme solution in the *PF**, $\overline{d}$ denotes average Euclidean distance of all the Pareto optimal solutions *PF* found.

- HV and IGD quantify and encapsulate both the convergence and diversity of the obtained *PF*, while HV requires a pre-defined reference point *R* and IGD relies on *PF**. Specifically, $HV(PF,R) = volume\left(\bigcup_{i=1}^{|PF|} v_i\right)$, where *R* is the worst objective values from all solutions obtained in all runs, v_i is a hypercube that is constructed with the reference point and the solution i in obtained *PF*. And $IGD = \frac{\sum_{x \in PF^*} d^{\min}(x,PF)}{|PF^*|}$, where $d^{\min}(x,PF)$ is the minimum Euclidean distance between the true Pareto optimal solution and solution in obtained *PF*, $|PF^*|$ is the non-dominated solution numbers.

The lower SP and IGD values are desirable, while a larger HV is better. Since the *PF** of our I-MACRP model is unknown, it is estimated by large-scale experiments (50 runs) on all compared algorithms, which is widely adopted to acquire *PF** of a real-world problem in the literature.

4.3 | Experimental results and analyses

4.3.1 | Metrics results analyses

Numerical comparison

Based on the above settings, the metric results of all compared algorithms on solving the I-MACRP model among 10 runs are summarized in Table 6, including mean, standard deviation (Std.), and median (Med.), and the best results are highlighted in boldface. We can find that our

ASTMOPSO algorithm has an excellent ability to find uniformly distributed and convergent solutions regardless of the instance scales. On the small scale (Scale = 4), it only exists a slight advantage over the second-rank NSGA-III algorithm. With the increment of instance scale, the benefit becomes obviously, since it increases by nearly 19%[1] (IGD), 12%(HV) on the medium scale (Scale = 9), and 33%(IGD), 18%(HV) on the large scale (Scale = 17), respectively. Regarding Pareto solutions distributivity (SP metric), all algorithms perform similarly without difference in each run. Besides, the original MOPSO performs worse than NSGA III while our ASTMOPSO algorithm performs better, which declares that our proposed seeking and tracking swarm strategies indeed improve convergence and overall performance on solving the model.

Statistic test

Furthermore, statistical tests are also given in Table 6. Wilcoxon's rank-sum test (Fay & Proschan, 2010) with a significance level of 0.05 is adopted to test the superiority credibility of our proposed ASTMOPSO over each of the other compared algorithms. Symbols '+', '−', and '≈' marked in the Med. columns indicate that the compared algorithm is significantly better than, worse than, or similar to our ASTMOPSO, respectively. As seen from Table 6, ASTMOPSO shows no statistically significant inferiority compared to any of the comparison algorithms in terms of distribution and convergence. This is evident from the absence of any symbol '+' across all metrics (IGD, HV, and SP). Specifically, for small and medium scales, NSGA-III exhibits similar solution effectiveness to our proposed algorithm, as indicated by statistically comparable performance. However, when considering large-scale problems, substantial performance differences become apparent. Analysis of the SP column reveals a

TABLE 6 Metrics results (GD, HV, and SP) on the I-MACRP model.

	Metrics								
	IGD			HV			SP		
Algorithms	Mean	Std.	Med.	Mean	Std.	Med.	Mean	Std.	Med.
Scale 4 (Small scale)									
SPEA 2	3765	242.9	3833^{-}	0.598	0.009	0.594^{-}	**1.00**	4.14e-06	**1.00**$^{\approx}$
MOPSO	3297	314.9	3166^{-}	0.621	0.014	0.627^{-}	**1.00**	4.05e-06	**1.00**$^{\approx}$
MOEA/D	4194	408.2	4099^{-}	0.540	0.039	0.542^{-}	**1.00**	5.62e-06	**1.00**$^{\approx}$
NSGA-III	1796	342.6	**1691**$^{\approx}$	0.747	0.031	0.755$^{\approx}$	**1.00**	9.09e-07	**1.00**$^{\approx}$
CMOPSO	3948	383.9	4011^{-}	0.581	0.016	0.577^{-}	**1.00**	3.85e-06	**1.00**$^{\approx}$
MORBCO	4026	285.6	3985^{-}	0.574	0.022	0.581^{-}	**1.00**	2.82e-06	**1.00**$^{\approx}$
ASTMOPSO	**1787**	**105.0**	1777	**0.757**	**0.007**	**0.756**	**1.00**	**4.41e-07**	**1.00**
+/−/≈	/	/	0/5/1	/	/	0/5/1	/	/	0/0/6
Scale 9 (Medium scale)									
SPEA 2	5780	**489.8**	5628^{-}	0.578	**0.016**	0.587^{-}	**0.99**	1.67e-06	**0.99**$^{\approx}$
MOPSO	7019	852.9	6699^{-}	0.560	0.017	0.565^{-}	1.00	**1.66e-06**	1.00$^{\approx}$
MOEA/D	7946	1248	8187^{-}	0.507	0.040	0.499^{-}	1.00	4.07e-06	1.00$^{\approx}$
NSGA-III	3861	1319	3591$^{\approx}$	0.614	0.030	0.618^{-}	1.00	1.76e-06	1.00$^{\approx}$
CMOPSO	8648	1122	8359^{-}	0.520	0.031	0.524^{-}	**0.99**	2.09e-06	**0.99**$^{\approx}$
MORBCO	8349	1180	8492^{-}	0.504	0.023	0.492^{-}	1.00	1.82e-06	1.00$^{\approx}$
ASTMOPSO	**3105**	1293	**3035**	**0.688**	0.048	**0.684**	1.00	4.33e-06	1.00
+/−/≈	/	/	0/5/1	/	/	0/6/0	/	/	0/0/6
Scale 17 (Large scale)									
SPEA 2	6160	2655	5390^{-}	0.444	0.039	0.446^{-}	**1.00**	1.95e-06	**1.00**$^{\approx}$
MOPSO	8957	1089	8870^{-}	0.394	0.020	0.397^{-}	**1.00**	1.11e-06	**1.00**$^{\approx}$
MOEA/D	10,454	3020	10,368^{-}	0.343	0.048	0.344^{-}	**1.00**	**3.88e-07**	**1.00**$^{\approx}$
NSGA-III	4367	1431	4130^{-}	0.513	0.026	0.513^{-}	**1.00**	5.55e-07	**1.00**$^{\approx}$
CMOPSO	14,845	1772	14,985^{-}	0.283	**0.019**	0.278^{-}	**1.00**	1.04e-06	**1.00**$^{\approx}$
MORBCO	10,571	2814	11,521^{-}	0.331	0.051	0.338^{-}	**1.00**	4.11e-07	**1.00**$^{\approx}$
ASTMOPSO	**2919**	**926.3**	**2953**	**0.606**	0.026	**0.615**	**1.00**	8.58e-07	**1.00**
+/−/≈	/	/	0/6/0	/	/	0/6/0	/	/	0/0/6

Note: /, no value needs to be recorded.

similar distribution pattern among all algorithms, potentially attributed to the sparsity of the feasible solution space in our high-dimensional constrained problem.

4.3.2 | Solution structure analyses

The numerical statistics discussed above provide convincing results but lack an intuitive comparison. In order to visualize the solution sets obtained by different algorithms, we plot the best performance solution found in 10 runs in Figure 3 for different instance scales. Note that deviation of duty time among crews f_1 and recovery cost f_2 are minimum objectives. Therefore, Pareto front should be as far to the lower left as possible. Experimental results in Figure 3 further confirm that ASTMOPSO has an overall better convergence performance than the other six compared algorithms. Since the proposed I-MACRP model is a multi-objective problem, it is better to find more solutions to balance all objectives in different situations discretionarily. From the figures, the most solution quantity found for different scales are 11 (it is found by SPEA 2 and ASTMOPSO finds 4 solutions which is only better than MOEA/D), 14 (it is found by ASTMOPSO and followed by the second rank 8 solutions found by MOPSO), and 14 (it is found by ASTMOPSO and followed by the second rank 11 solutions found by MORBCO). Our ASTMOPSO algorithm seems to have better solution-finding ability than the other algorithms when the instance scale is large.

4.3.3 | Further discussions

Discussion on infeasible solution repair procedures

Since our I-MACRP model is a complex multi-objective problem with various constraints, it is difficult to find a feasible solution. To demonstrate the effectiveness of our proposed repair methods (as shown in Section 3.1) in finding the feasible solution, we focus on the feasible rate (FR), which is the ratio of the number of feasible runs to the total number of runs. Our five repair procedures focus on variable boundary handling (procedure 1), crew constraint handling (procedure 2), and time constraint (procedures 3 to 5) handling. Since repair procedure 1 has been adopted popularly in literature, we delete repair procedures 2 and 3 to do further discussion for our ASTMOPSO algorithm. The comparisons of ASTMOPSO-noC (without procedure 2), ASTMOPSO-noT (without procedure 3), ASTMOPSO-noC&T (without both procedures 2 and 3) with ASTMOPSO in terms of FR are shown in Table 7, where the best results are in boldface. We can find that our ASTMOPSO considering repair methods on crew and time can obtain feasible solutions in all 10 runs on all instances. Its significant advantage in finding feasible solutions is that a set of constraints is checked and satisfied in each step during the solution construction. In contrast, neglecting adjustment on crew or time only has a nearly 40% probability of finding a feasible solution in all scale instances. As more repair methods are neglected (ASTMOPSO-noC&T), the smaller FR can hardly obtain a feasible solution in large scale with a high dimensional search space.

Discussion on cruise speed recovery action

Table 8 compares the recovery performance between considering cruise speed control recovery (CSC) and no cruise speed control recovery action (N-CSC). It takes one of Pareto solutions found by ASTMOPSO algorithm as an example and the results of N-CSC case can be acquired easily by setting $v_{f_{s,j}} = \underline{v}_{f_{s,j}}$. For each scale, the last row calculates the improvement of the CSC-considered algorithm compared to its corresponding N-CSC case. Table 7 shows that adopting cruise speed control as a recovery action helps reduce disturbed flights and total delay time, which is helpful in comforting the emotion of stakeholders. This is because the aircraft under CSC situation can speed up to arrive before airport closure or satisfy minimal ground turn-around time requirement, which significantly declines delay to downstream flights.

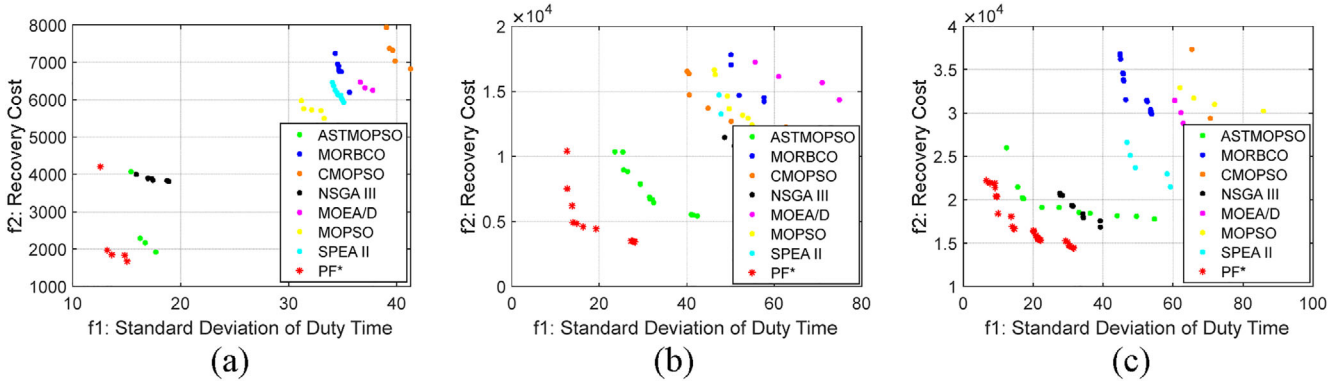

FIGURE 3 Pareto front of all algorithms for different instance scales. (a) small scale; (b) medium scale; (c) large scale.

TABLE 7 Comparison of FR results under different ASTMOPSO variants.

Variants scale	ASTMOPSO-noC	ASTMOPSO-noT	ASTMOPSO-noC&T	ASTMOPSO
4	60%	40%	30%	**100%**
9	50%	40%	10%	**100%**
17	40%	30%	0%	**100%**

TABLE 8 Comparison of recovery results under CSC and N-CSC cases.

	Feasibility	No. delay flights	Total delay time
Scale 4 (Small scale)			
CSC	Yes	8	203
N-CSC	Yes	11	291
Improvement	/	27.27%	30.24%
Scale 9 (Medium scale)			
CSC	Yes	19	666
N-CSC	Yes	21	795
Improvement	/	9.52%	16.23%
Scale 17 (Large scale)			
CSC	Yes	45	3591
N-CSC	Yes	48	4067
Improvement	/	6.25%	11.70%

4.3.4 | Recovery scheme exhibition

One illustrative recovery scheme on the instance provided by the ASTMOPSO algorithm is presented in Figure 4. The planned and recovered schemes for each disturbed flight are shown in grey and orange rectangles, respectively (the grey rectangle will be neglected if no timetable and cruise speed change). Their decision deviations on delay time, cruise speed, and crew re-arrangement introduced in Sect. 3.2 are depicted by the 3-dimension data above the orange rectangle. For example, (0,0,6) above the orange rectangle $f_{1,1}$ means that the first flight in string 1 keeps its departure time and cruise speed, and it will be operated by crew 6. In this recovery scheme, the actual earliest off-duty string is $f_{1,1} \rightarrow f_{1,2}$ and it will be executed by corresponding winner crew 6. From Figure 4, the flights $f_{1,2}, f_{8,2}$ and $f_{9,2}$ are successful in avoiding the influence of airport closure by increasing cruise speed to go back to the base airport before the closure time. Reserve crews 14, 15, and 20 are called on this recovery scheme.

5 | CONCLUSIONS AND FUTURE WORKS

Unlike most existing I-ACRP models that only consider costs from airlines, this study proposes a new multi-objective model from both airlines and crew perspectives. Precisely, crew satisfaction is measured by on-duty time difference and preference for the earliest off- duty task through bidding. Besides, a novel ASTMOPSO algorithm is developed to efficiently solve the multi-objective model. Two adaptive swarms with improved evolutionary strategies are employed to balance the abilities between global detection and local search. And five ad-hoc infeasible solution repair procedures are proposed to increase the probability of finding feasible solutions.

Experiments conducted on three instances from real world verify the effectiveness of our ASTMOPSO in solving the proposed I-MACRP model. ASTMOPSO statistically outperforms the other compared optimization algorithms and the infeasible solution repair procedures significantly improve the feasibility rate by at least 40%, particularly for large-scale instances.

Our proposed model and optimizer try to give high-quality recovery schemes for integrated aircraft and crew suffering airport closure. Since the timetable and crew are mixed decision variables, our encoding strategy is also helpful in other practical problems. The present work is limited to single-day recovery; however, severe airport closures can result in disruptions spanning multiple days. Therefore, in future research, we will focus on studying multi-day recovery. Additionally, passenger recovery serves as the final stage of restoring operations after disruptions, and integrating it into our future studies to achieve holistic recovery would be an intriguing topic.

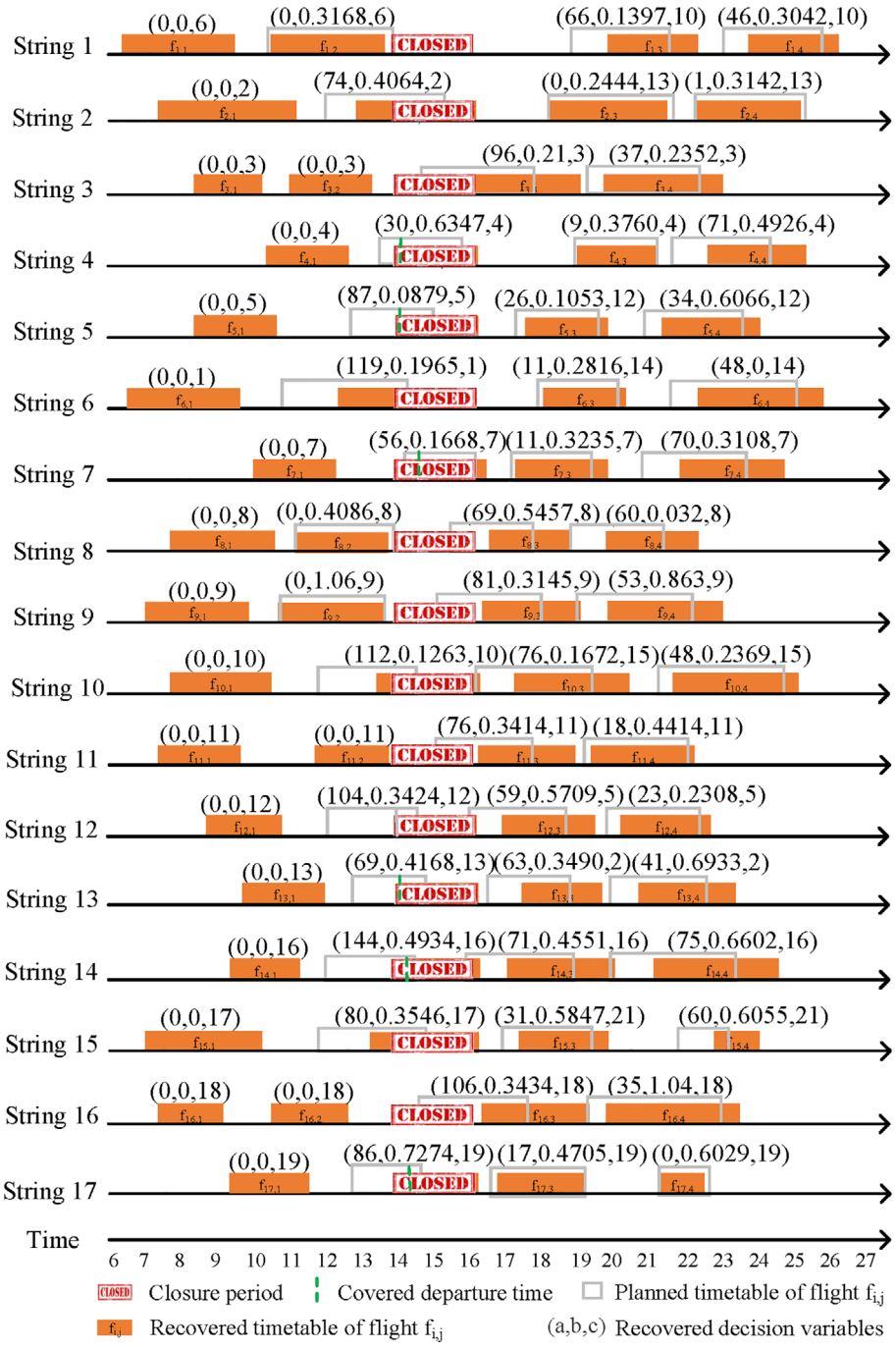

FIGURE 4 One of recovery scheme for the I-MACRP model.

ACKNOWLEDGEMENTS

The authors would like to thank VariFlight Company for providing operational data from Shenzhen Airline and Shenzhen University for technical support.

FUNDING INFORMATION

The work described in this paper is supported in part by the National Natural Science Foundation of China (Nos. 62103286, 71971143); in part by the Humanities and Social Sciences Youth Foundation, Ministry of Education of the People's Republic of China under Grant (No. 21YJC630181); in part by the Grant of University of Macau (No. MYRG2019-00031-FBA); in part by the Guangdong Provincial Philosophy and Social Sciences Planning Project (No. GD22XGL22, GD22CGL35), in part by the Special Projects in Key Fields of Universities in Guangdong Province (No. 2022ZDZX2054); in part by the Guangdong Province Innovation Team (No. 2021WCXTD002); in part by the Basic and Applied

Basic Research Foundation of Guangdong Province (No. 2019A1515110401); in part by the Natural Science Foundation of Guangdong Province (No. 2020A1515010752); and in part by the Natural Science Foundation of Shenzhen City (No. JCYJ20190808145011259).

CONFLICT OF INTEREST STATEMENT

The authors declare no conflicts of interest.

DATA AVAILABILITY STATEMENT

Data sharing not applicable to this article as no datasets were generated or analysed during the current study.

ORCID

Huifen Zhong https://orcid.org/0000-0002-7968-7743
Zhaotong Lian https://orcid.org/0000-0002-0408-4382
Tianwei Zhou https://orcid.org/0000-0003-3533-7204
Ben Niu https://orcid.org/0000-0001-5822-8743
Bowen Xue https://orcid.org/0000-0001-8673-706X

ENDNOTE

[1] $19\% = (3861 - 3105)/3861 \times 100\%$. A similar calculation can be applied to the other results.

REFERENCES

Achour, H., Gamache, M., Soumis, F., & Desaulniers, G. (2007). An exact solution approach for the preferential bidding system problem in the airline industry. *Transportation Science*, *41*(3), 354–365.

Aguiar, B., Torres, J., & Castro, A. J. (2011). Operational problems recovery in airlines–a specialized methodologies approach. In *Progress in Artificial Intelligence* (pp. 83–97).

Arıkan, U., Gürel, S., & Aktürk, M. S. (2017). Flight network-based approach for integrated airline recovery with cruise speed control. *Transportation Science*, *51*(4), 1259–1287.

Atencia, C. R., Del Ser, J., & Camacho, D. (2019). Weighted strategies to guide a multi-objective evolutionary algorithm for multi-UAV mission planning. *Swarm and Evolutionary Computation*, *44*, 480–495.

Azouz, Y., & Boughaci, D. (2022). Multi-objective memetic approach for the optimal web services composition. *Expert Systems*, *e13084*, 1–28.

Ben Ammar, H., Ayadi, O., & Masmoudi, F. (2020). An effective multi-objective particle swarm optimization for the multi-item capacitated lot-sizing problem with set-up times and backlogging. *Engineering Optimization*, *52*(7), 1198–1224.

Bosman, P. A., & Thierens, D. (2003). The balance between proximity and diversity in multiobjective evolutionary algorithms. *IEEE Transactions on Evolutionary Computation*, *7*(2), 174–188.

Chen, C. H., Liu, T. K., & Chou, J. H. (2013). Integrated short-haul airline crew scheduling using multiobjective optimization genetic algorithms. *IEEE Transactions on Systems, Man, and Cybernetics: Systems*, *43*(5), 1077–1090.

Coello, C. A. C., Pulido, G. T., & Lechuga, M. S. (2004). Handling multiple objectives with particle swarm optimization. *IEEE Transactions on Evolutionary Computation*, *8*(3), 256–279.

Cook, A., Tanner, G., Williams, V., & Meise, G. (2009). Dynamic cost indexing–managing airline delay costs. *Journal of Air Transport Management*, *15*(1), 26–35.

Deb, K., & Jain, H. (2013). An evolutionary many-objective optimization algorithm using reference-point-based nondominated sorting approach, part I: Solving problems with box constraints. *IEEE Transactions on Evolutionary Computation*, *18*(4), 577–601.

Deb, K., Pratap, A., Agarwal, S., & Meyarivan, T. A. M. T. (2002). A fast and elitist multiobjective genetic algorithm: NSGA-II. *IEEE Transactions on Evolutionary Computation*, *6*(2), 182–197.

Del Ser, J., Osaba, E., Molina, D., Yang, X. S., Salcedo-Sanz, S., Camacho, D., & Herrera, F. (2019). Bio-inspired computation: Where we stand and what's next. *Swarm and Evolutionary Computation*, *48*, 220–250.

Dou, J., Li, J., Xia, D., & Zhao, X. (2021). A multi-objective particle swarm optimisation for integrated configuration design and scheduling in reconfigurable manufacturing system. *International Journal of Production Research*, *59*(13), 3975–3995.

Erdem, E., Aydın, T., & Erkayman, B. (2021). Flight scheduling incorporating bad weather conditions through big data analytics: A comparison of metaheuristics. *Expert Systems*, *38*(8), e12752.

Fay, M. P., & Proschan, M. A. (2010). Wilcoxon-Mann-Whitney or t-test? On assumptions for hypothesis tests and multiple interpretations of decision rules. *Statistics Surveys*, *4*, 1–39.

Gamache, M., Soumis, F., Villeneuve, D., Desrosiers, J., & Gélinas, É. (1998). The preferential bidding system at air Canada. *Transportation Science*, *32*(3), 246–255.

Hassan, L. K., Santos, B. F., & Vink, J. (2021). Airline disruption management: A literature review and practical challenges. *Computers & Operations Research*, *127*, 105137.

Jordehi, A. R. (2015). A review on constraint handling strategies in particle swarm optimisation. *Neural Computing and Applications*, *26*, 1265–1275.

Khiabani, A., Rashidi Komijan, A., Ghezavati, V., & Mohammadi Bidhandi, H. (2022). A mathematical model for integrated aircraft and crew recovery after a disruption: A Benders' decomposition approach. *Journal of Modelling in Management*.

Le, M. L., & Wu, C. C. (2013). Solving airlines disruption by considering aircraft and crew recovery simultaneously. *Journal of Shanghai Jiaotong University (Science)*, *18*, 243–252.

Maenhout, B., & Vanhoucke, M. (2010). A hybrid scatter search heuristic for personalized crew rostering in the airline industry. *European Journal of Operational Research*, *206*(1), 155–167.
Maher, S. J. (2016). Solving the integrated airline recovery problem using column-and-row generation. *Transportation Science*, *50*(1), 216–239.
Nayak, J., Mishra, M., Naik, B., Swapnarekha, H., Cengiz, K., & Shanmuganathan, V. (2022). An impact study of COVID-19 on six different industries: Automobile, energy and power, agriculture, education, travel and tourism and consumer electronics. *Expert Systems*, *39*(3), e12677.
Niu, B., Liu, Q., Wang, Z., Tan, L., & Li, L. (2021). Multi-objective bacterial colony optimization algorithm for integrated container terminal scheduling problem. *Natural Computing*, *20*, 89–104.
Nuic, A. (2010). User manual for the Base of Aircraft Data (BADA) revision 3.10. Atmosphere, 2010, 001.
Pejovic, T., Noland, R. B., Williams, V., & Toumi, R. (2009). A tentative analysis of the impacts of an airport closure. *Journal of Air Transport Management*, *15*(5), 241–248.
Petersen, J. D., Sölveling, G., Clarke, J. P., Johnson, E. L., & Shebalov, S. (2012). An optimization approach to airline integrated recovery. *Transportation Science*, *46*(4), 482–500.
Poles, D. (2009). Base of aircraft data (BADA) aircraft performance modelling report. *EEC Technical/Scientific Report*, *9*, 1–68.
Quesnel, F., Wu, A., Desaulniers, G., & Soumis, F. (2022). Deep-learning-based partial pricing in a branch-and-price algorithm for personalized crew rostering. *Computers & Operations Research*, *138*, 105554.
Su, Y., Xie, K., Wang, H., Liang, Z., Chaovalitwongse, W. A., & Pardalos, P. M. (2021). Airline disruption management: A review of models and solution methods. *Engineering*, *7*(4), 435–447.
Tan, W., Yuan, X., Huang, G., & Liu, Z. (2021). Low-carbon joint scheduling in flexible open-shop environment with constrained automatic guided vehicle by multi-objective particle swarm optimization. *Applied Soft Computing*, *111*, 107695.
Wu, C. L., & Caves, R. E. (2002). Modelling of aircraft rotation in a multiple airport environment. *Transportation Research Part E: Logistics and Transportation Review*, *38*(3–4), 265–277.
Zhang, D., Lau, H. H., & Yu, C. (2015). A two stage heuristic algorithm for the integrated aircraft and crew schedule recovery problems. *Computers & Industrial Engineering*, *87*, 436–453.
Zhang, Q., & Li, H. (2007). MOEA/D: A multiobjective evolutionary algorithm based on decomposition. *IEEE Transactions on Evolutionary Computation*, *11*(6), 712–731.
Zhang, X., Zheng, X., Cheng, R., Qiu, J., & Jin, Y. (2018). A competitive mechanism based multi-objective particle swarm optimizer with fast convergence. *Information Sciences*, *427*, 63–76.
Zhou, S. Z., Zhan, Z. H., Chen, Z. G., Kwong, S., & Zhang, J. (2020). A multi-objective ant colony system algorithm for airline crew rostering problem with fairness and satisfaction. *IEEE Transactions on Intelligent Transportation Systems*, *22*(11), 6784–6798.
Zitzler, E., Laumanns, M., & Thiele, L. (2001). SPEA2: Improving the strength Pareto evolutionary algorithm. TIK-report, 103.
Zitzler, E., & Thiele, L. (1999). Multiobjective evolutionary algorithms: A comparative case study and the strength Pareto approach. *IEEE Transactions on Evolutionary Computation*, *3*(4), 257–271.
Zomorodi-Moghadam, M., Abdar, M., Davarzani, Z., Zhou, X., Pławiak, P., & Acharya, U. R. (2021). Hybrid particle swarm optimization for rule discovery in the diagnosis of coronary artery disease. *Expert Systems*, *38*(1), e12485.

AUTHOR BIOGRAPHIES

Huifen Zhong received the B.S. degree in Decision Science from School of Management, Guangdong University of Technology, Guangzhou, China, in 2016, the M.S. degree in Management Science and Engineering, Guangdong University of Technology, Guangzhou, China, in 2019. She is currently pursuing her Ph. D degree in University of Macau, Macau, China. Her research interests focus on Intelligence Computing, Constrained Multi-objective Optimization, and Transportation Scheduling.

Zhaotong Lian is a full professor at the Faculty of Business Administration, University of Macau. Prof. Lian received his Ph. D in Operations Management from Hong Kong University of Science and Technology. His research interests are Stochastic Models, Business Analytics, Supply Chain and Service Management. He has published many research papers in outstanding journals, including Operations Research, Production and Operations Management, Mathematics of Operations Research, Naval Research and Logistics (2 UTD, 1 ABS4*, 8 ABS4 and 18 ABS3).

Tianwei Zhou received the B.S. degree in automation and the Ph.D. degree in control science and engineering from Tianjin University, Tianjin, China, in 2014 and 2019, respectively. She was a joint Ph.D. student with the Department of Electrical and Computer Engineering, National University of Singapore, Singapore, from August 2017 to August 2018. She is currently an Assistant Professor with the College of Management, Shenzhen University, Shenzhen, China. Her current research interests include intelligent scheduling and event-triggered control.

Ben Niu received his Ph. D degree from Shenyang Institute of Automation of the Chinese Academy of Sciences, Shenyang, China, in 2008. In 2008, he joined the College of Management, Shenzhen University, Shenzhen, China, where he is currently a Full Professor. He was a Visiting Scholar with the University of Edinburgh, Arizona State University, Victoria University of Wellington, Hong Kong University in 2018, 2016, 2013, and 2011. During 2013 to 2016, he worked as a Postdoctoral Research Fellow with the Hong Kong Polytechnic University. His research interests include Operations Research and Optimization, Artificial Intelligence, Big Data Analysis and Processing, Smart Healthcare, etc.

Bowen Xue obtained the B.S. degree from Business School at Shandong Normal University, Ji'nan, China. She received the M. S degree in Management Science and Engineering from College of Management at Shenzhen University, Shenzhen, China. She is going to pursue her Ph. D degree in the University of Manchester, Manchester, UK. Her current research activities focus on improving and applying bio-inspired computing to scheduling optimization problems and reinforcement learning, developing optimization and simulation models for green supply chain management.

How to cite this article: Zhong, H., Lian, Z., Zhou, T., Niu, B., & Xue, B. (2023). Integrated recovery system with bidding-based satisfaction: An adaptive multi-objective approach. *Expert Systems*, e13409. https://doi.org/10.1111/exsy.13409